energies

MDPI

Article

Non-Matrix Quick Pass: A Rapid Evaluation Method for Natural Fractures and Karst Features in Core

Paul J. Moore [1,*] and Fermin Fernández-Ibáñez [2]

[1] ExxonMobil Research Qatar, Doha, Qatar
[2] ExxonMobil Upstream Research Company, Houston, TX 77098, USA; fermin.fernandez.ibanez@exxonmobil.com
* Correspondence: pj.moore@exxonmobil.com

Abstract: Mechanical and chemical processes experienced by carbonate rocks result in a complex network of natural fractures and dissolution features that have direct implications on porosity, permeability, and connectivity in reservoirs. Characterization of natural fractures is best done in core; however, it can be time-consuming due to the large amounts of individual features present and the long list of attributes typically collected for each feature. Additionally, karst features in core, such as vugs and small cavities, are seldom characterized in a quantitative way or are overlooked. We introduce a new methodology, called the non-matrix quick pass (NMQP), which allows for the collection of non-matrix features in a rapid yet quantitative fashion at a rate of 12 to 20 m of core per hour. The NMQP methodology offers enough vertical resolution so that observations can be integrated with other wellbore data types (e.g., wireline logs, well tests, and production logs). This method also yields estimates of density and porosity that are rigorous enough to provide the technical basis to build first-generation dual-porosity models describing the non-matrix component of a carbonate reservoir and its potential impact on field performance.

Keywords: dual porosity; core logging; carbonate reservoir characterization; non-matrix characterization; karst; fractures

Citation: Moore, P.J.; Fernández-Ibáñez, F. Non-Matrix Quick Pass: A Rapid Evaluation Method for Natural Fractures and Karst Features in Core. *Energies* **2022**, *15*, 4347. https://doi.org/10.3390/en15124347

Academic Editors: Yuming Liu and Bo Zhang

Received: 22 March 2022
Accepted: 9 June 2022
Published: 14 June 2022

1. Introduction

Conventional core is a key dataset used to understand the geologic processes occurring within a reservoir. The wealth of information gained comes from observations made on the core and subsequent analyses done on core samples. Geologic descriptions from core focus on understanding how the processes of sedimentology, stratigraphy, and chemical and mechanical diagenesis have evolved over time [1,2]. Such observations typically evaluate changes in rock fabric, grain size and sorting, stacking patterns, porosity, and structural discontinuities. This information is critical in deciphering the geologic history of a reservoir, such as developing a sequence stratigraphic framework or modeling the intensity and distribution of natural fractures [3,4].

In carbonate reservoirs and aquifers, geologic core has been instrumental in addressing the complexity of the carbonate pore system, which can be separated into two main categories of matrix and non-matrix porosity. Matrix porosity is represented by pore types that are equal to or smaller than the surrounding host grains. The matrix pore system has been studied using core by a number of methods, including by classifying pore types by genetic origin [5], differentiating pore types by connectivity of the pore space [6,7], relating pore space to petrophysical rock properties [8–11], characterizing pore throat size and distributions [12,13], quantifying pore types and geometries [14–17], and characterizing and defining microporosity [18–24].

In contrast to matrix porosity, non-matrix porosity is represented by pore types that are larger than the surrounding host grains and can extend several orders of magnitude larger in size compared to matrix pores. The two processes responsible for non-matrix porosity are

through the development of natural fractures and karstification, which results in features including joints, faults, touching vugs, and caves. Although the multiscale nature of the non-matrix pore system often requires multiple datasets for proper characterization [25,26], there is a wealth of knowledge to be gained from utilizing geologic core for characterizing fractures and karst because of the ability to address the processes responsible for their development [25–34]. For example, Tinker et al. [25] utilized more than 8500 m of core and complimentary wireline logs to quantify the contribution of karst porosity within the Permian Yates field in southwest Texas, USA. Ibrayev et al. [34] used a combination of static (e.g., core, wireline, and image) and dynamic (e.g., drilling data and well tests) datasets to develop a genetic-based understanding of fracture development in the Carboniferous Kashagan field in the North Caspian offshore, Kazakhstan. Ahdyar et al. [26] incorporated static (core, wireline, image, and 3D seismic) and dynamic (drilling data, production logs, and pressure transient analysis) datasets to characterize the distribution and pore volume associated with non-matrix processes within the Oligo-Miocene Banyu Urip field onshore, Indonesia.

Non-matrix features are often observed and described in core [28,30,34]; however, typically, only the fracture portion of the non-matrix pore system is cataloged in a systematic way that addresses fracture geometries and spacing [33,35]. Although karst features are commonly recognized in core, such observations are rarely cataloged along with and in addition to the fracture observations to understand the impact that these combined features may have on the non-matrix pore system. Instead, observations of karst features are often used to support the building of a sequence stratigraphic framework or to understand the diagenetic processes that likely occurred in the reservoir [30,36,37]. Nonetheless, the non-matrix pore system is a combination of chemical and mechanical processes that often occur in similar locations, e.g., along the margin of carbonate platforms. Consequently, in order to be predict the magnitude and distribution of all non-matrix features and their associated pore volume within a given field, systematic cataloging of these different non-matrix features is warranted.

In this paper, we present a methodology that arose from the need to collect an integrated karst and fracture dataset from a large amount of core in multiple wells, i.e., total lengths in excess of 5000 m per study. We were tasked with collecting quantitative data from non-matrix features observed in cores that could be used for reservoir characterization and development of initial geologic concepts. The description of such large amounts of core had to be achieved using a rapid yet adequate quantitative data collection strategy so that business deadlines could be met while ensuring the technical integrity of our work. Therefore, detailed data collections strategies such as those employed in traditional fracture characterization [2] were not an option, as they cover less than about 20 m of core per day [38,39]. The data collected should also be quickly processed and suitable for integration with other wellbore-based datasets (e.g., drilling data, wellbore images, wireline logs, and seismic and production data) while providing some basic inputs for geostatistical reservoir models. The fast and quantitative yet simple data collection approach allows a team of two to cover more than 100 m of core in less than two days of work. The final methodology described herein has been successfully implemented as standard practice for the characterization of non-matrix in cores collected in several carbonate reservoirs that we have worked. Obviously, non-matrix observations collected using this method are not free of sampling bias inherent to core. For example, bias due to fracture spacing and the likelihood of intersecting a fracture must be considered [40,41].

2. Methodology and Workflow

Non-matrix quick pass (NMQP) is based on a set of rules and methodologies that ensures consistency within and between cored wells. This workflow was developed based on a balance between time spent on the core and ensuring that sufficient observations were made and recorded to capture the variability in non-matrix features observed in core, which can be used to compliment additional datasets. This method does not replace detailed

data collection. Instead, it provides a means for describing large amounts of core that can identify specific areas for further detailed work. The methodology is designed to be run in teams of two. Although each individual reports on the observable non-matrix features, one person is tasked with measuring (i.e., quantifying) each feature, and the other person inputs the data directly in a computer.

2.1. Ground Rules

In order to ensure consistency, the first step of the data collection process is to establish some ground rules and clearly define how the data will be collected, as well as the amount of detail required to meet the objectives of the study. The list below highlights some key rules that we have found useful in collecting the appropriate amount of detail while optimizing the time spent on each core interval described with the NMQP methodology:

1. Always utilize the whole core whenever possible, i.e., use both sides of a slabbed core to ensure maximum core coverage. Refrain from using core photos. Most core descriptions are performed on a 1/3 slabbed portion. Although this portion of the core is sufficient for making observations on sedimentology, NMQP works best if non-matrix observations are made on the 2/3 portion of the core. The logic is simple. The larger sample size allows for the recognition of non-matrix features that are often under-sampled in the 1/3 portion. We have also found that many non-matrix features are often found on the backside of the core due to the core being slabbed to avoid intersecting non-matrix features that can compromise the integrity of the 1/3 slabbed portion. In the case of fractures, the spacing, orientation, and angle of the fracture with respect to the core can lead to significant sampling bias.
2. Define a collection interval. For simplicity, we use the length of core that fits in the box used to store the core. This length is usually one meter and provides enough resolution to identify trends and intervals of interest for further analyses or data collection. Alternatively, the user can define custom intervals that could be driven by lithologic or mechanically distinctive units or simply a smaller regular interval for higher-resolution results.
3. Evaluate the integrity and layout of the core. This step is meant to account for core handling and previous sampling efforts, which can create issues with core quality, incorrect orientation (e.g., upside-down core), mislabeled core boxes, and missing core. Core integrity is also a flag for reliability or confidence with respect to the collected data, analysis, and derived results. In our experience, non-matrix features are easily overlooked when core integrity is low. Low core integrity can result from the presence of non-matrix features but also from poor core handling or drilling operations.
4. Define a target maximum amount of time to be spent on each interval (or core box). We have determined that no more than five minutes per core box (assuming one meter) is a target sufficient to capture the proper amount of information. Of course, there might be core intervals with a large amount of features and complex relationships that might require more than the maximum specified time, and this is appropriate as long as the majority of the core intervals are completed within five minutes. If the analysts spends more than an average of five minutes per interval, too much detail is being collected and perhaps the ground rules need to be revisited. Figure 1 shows the distribution of times spent collecting data in more than 300 boxes of core with different levels of non-matrix abundance and complexity. On average, we spent just under three minutes to collect all the information we deemed necessary in a typical interval. Boxes that took longer than five minutes usually corresponded to a high density of non-matrix features or low core integrity, which required some degree of core reconstruction. The time per interval reported in Figure 1 includes data collected by different analysts with varying degrees of experience with the NMQP methodology.
5. Define a minimum size and amount of features to be characterized. We typically log only fractures that are >2 cm in length with apertures $\geq$0.05 mm and more than 10 cm cumulative length per box. In the case of karst features, we only log features that are

>1 cm^2 with evidence of dissolution, i.e., molds and other depositional pores, such as fenestrae, are excluded. For simplicity in the NMQP, we refer to any dissolution-enhanced pore as a vug. A touching vug implies that multiple dissolution-enhanced vugs are connected in the core [42]. The lower limits of recorded observations, e.g., vug >1 cm^2 and fractures >2 cm in length, were set to increase efficiency while on the core. The main idea here is that smaller features, regardless of abundance, are not expected to significantly contribute to the non-matrix pore system flow.

6. Agree on the threshold between fracture and karst feature. Although this might be an overstatement, we have run into many situations where fractures are enhanced so much by dissolution that they develop vug-like aspect ratios (e.g., Figure 4C in [43]). Therefore, it is critical to make appropriate observations on cross-cutting relationships, such as by establishing whether a vug was intersected by a fracture or developed along a fracture. In any case, do not capture the same observation twice, i.e., classify as both fracture and karst.

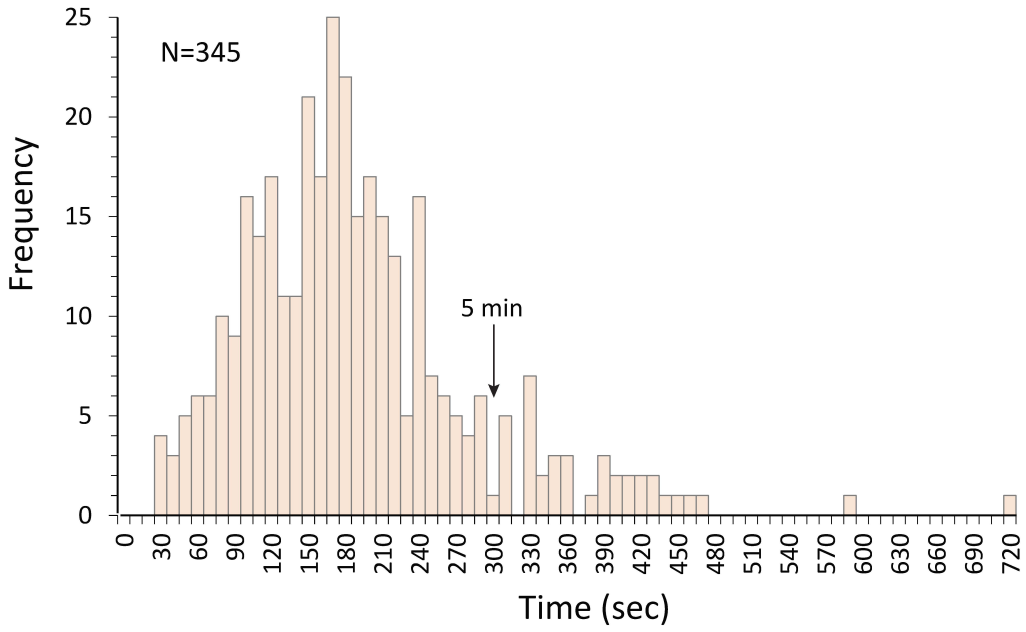

Figure 1. Histogram showing the distribution of time spent collecting non-matrix observations on more than 345 boxes of core using the NMQP method.

2.2. Data Collection

Measuring tape, a small ruler or a comparator [43], a hand lens, a computer, and a clean core surface are the minimum requirements to get started. Figure 2 illustrates the spreadsheet format we use to collect the information that is reported during an NMQP. Data are easily recorded using an alphanumerical system that can easily be translated into other software packages optimized for well log analysis. Table 1 shows an example key that can be used to record information in the spreadsheet. With a bit of practice, the alphanumeric key can be easily remembered by analysts, which reduces the time spent on each interval. Each row in the spreadsheet represents a single core box. For each core box, the top and base of the interval are recorded, along with the core dimensions, which include the core diameter and cut, such as the 1/3 or 2/3 portion of the slabbed core. Core integrity is typically input on this first pass of the core, together with the top and bottom of each interval (or core box). The core integrity scale ranges from 1 to 5 (Figure 3). Once the depth, dimensions, and quality of the core have been captured, each core box is evaluated for the presence of fractures and karst features.

Box	Depth		Core Dimensions		Core Integrity	Fractures								Karst						
	Top	Base	Width	Cut		Type	Count	$\Sigma_{lengths}$	Width		Distribution	Openness	Fill	Type	Count	Size		Distribution	Openness	Fill
	(m)	(m)	(cm)	(slab)			(min)	(cm)	Avg (mm)	Max (mm)						Avg (cm^2)	Max (cm^2)			
1	1910.00	1910.91	10	2/3	5	-	-	-	-	-	-	-	-	-	-	-	-	-	-	-
2	1910.92	1911.79	10	2/3	5	-	-	-	-	-	-	-	-	-	-	-	-	-	-	-
3	1911.79	1912.70	10	2/3	5	2	10	40	0.05	0.05	1,2,3	0	1	4	2	3	4	3	3	2
4	1912.70	1913.56	10	2/3	5	2	3	30	0.05	0.2	2	0	1	4	1	5	5	1	4	2,7
5	1913.56	1914.46	10	2/3	5	-	-	-	-	-		-	-	3	2	6	6	1	1	1
6	1914.46	1915.37	10	2/3	5	2	5	25	0.1	1	3	0	2	-	-	-	-	-	-	-
7	1915.37	1916.27	10	2/3	5	2	5	70	0.1	0.1	1	0	1,2	-	-	-	-	-	-	-
8	1916.27	1917.18	10	2/3	2	2	3	75	0.1	0.1	2	0	1,6	7	4	18	24	1,2,3	1	2
9	1917.18	1918.12	10	2/3	3	-	-	-	-	-		-	-	-	-	-	-	-	-	-
10	1918.12	1918.98	10	2/3	3	2	5	110	0.05	0.1	1,2,3	1	1,6	-	-	-	-	-	-	-
11	1918.98	1919.89	10	2/3	4	2	1	10	0.1	0.2	1	0	1,6	-	-	-	-	-	-	-
12	1919.89	1920.81	10	2/3	5	2	8	160	0.05	0.1	1,2,3	0	1,2	-	-	-	-	-	-	-
13	1920.81	1921.72	10	2/3	3	-	-	-	-	-		-	-	4	2	18	32	2	3	1
14	1921.72	1922.63	10	*2/3*	3	-	-	-	-	-		-	-	-	-	-	-	-	-	-
15	1922.63	1923.48	10	2/3	5	2	2	50	0.05	0.05	1,2,3	0	2	5	1	30	30	1	3	2,7
16	1923.48	1924.31	10	2/3	5	1	1	12	1	6	1	0	4	-	-	-	-	-	-	-
17	1924.31	1925.19	10	2/3	5	-	-	-	-	-	-	-	-	-	-	-	-	-	-	-
18	1925.19	1926.10	10	2/3	3	-	-	-	-	-	-	-	-	-	-	-	-	-	-	-
19	1926.10	1927.00	10	2/3	4	2	4	75	0.05	1	3	1	1	5	1	40	40	2	0	1,2
20	1927.00	1927.90	10	2/3	4	-	-	-	-	-	-	-	-	4	1	42	42	1	2	2

Figure 2. Example of a spreadsheet format used in the NMQP methodology. A detailed explanation of the non-matrix metrics that are recorded is provided in the text.

Table 1. Example key of the alphanumerical system used in the NMQP methodology.

Core Integrity	Non-Matrix Types	Distribution	Openness	Fill
1–Rubble	1–1st Gen Fractures	1–Upper 1/3	0–Closed (<10%)	1–Bitumen
2–Rubble w/intact sections	2–2nd Gen Fractures	2–Middle 1/3	1–Slightly Open (10–30%)	2–Calcite cement
3–Partially intact *	3–Breccia	3–Lower 1/3	2–Partly Open (30–70%)	3–Clay
4–Mostly intact *	4–Vug		3–Mostly Open (70–90%)	4–Debris
5–Completely intact †	5–Touching Vugs		4–Open (>90%)	5–Anhydrite
	6–Vugs on Fracture			6–Stylolite residue
	7–Vug in breccia			7–Breccia clasts

* Can have missing pieces; † may be broken.

Figure 3. Examples showing variations in core integrity. (**A**) rubble, (**B**) rubble with intact sections, (**C**) partially intact, (**D**) mostly intact, (**E**) completely intact. Core intervals with missing pieces or being broken does not impact the core integrity call.

2.2.1. Fracture Metrics

In an ideal situation, some sort of fracture paragenesis work should have been done prior to collecting these data. This can be achieved by using geochemical techniques that analyze cement types and paragenesis or more simply by observing the type of cement fills and cross-cutting relationships. When a fracture paragenesis exists, the first step is to identify the genetic fracture types present in the analyzed interval. Genetic types refer

to the relative timing and processes responsible for fracture development, which also has implications for the type of fill that may be present. For example, early fractures that form contemporaneously with sediment deposition are commonly open at the surface [34]. Consequently, such fractures are often filled with carbonate debris and soil-derived clays. Conversely, late fractures that develop during burial often crosscut the early fractures and are filled with calcite cement. Conducting NMQP within a fracture-paragenetic sequence allows the user to distribute properties and fracture types in a model using a genetic-based approach. This effectively means being able to define areas with a higher probability of finding certain types of fractures and assigning different properties of each fracture generation. NMQP can also be performed in the absence of fracture paragenesis work; however, there will be uncertainty on understanding what controls fracture distribution within the reservoir. Regardless, NMQP can still be used to identify general distribution trends and sweet spots or make inferences about mechanical stratigraphy. The following fracture metrics should be collected independently for each fracture generation (or type):

- *Count*: number of fractures of a given genetic type that meet the conditions defined by the ground rules. When counting fractures, one should avoid counting the same fracture twice at the intersection with the slabbed face and the back of the core. The user should not forget that the number of fractures sampled by the core is highly dependent of fracture spacing and orientation; therefore, the core is only a partial representation of fractures in the subsurface.
- *Cumulative Length*: summation of all fracture trace lengths of the same fracture generation.
- *Characteristic width*: a rough estimate of an average or most representative width of each fracture type observed in the core interval. Width is defined as the distance from wall to wall of a given fracture, regardless of whether the fracture is filled or open. A simple measuring scale or comparator [44] can be used.
- *Maximum width*: the maximum observed width of a given fracture type. In reservoirs with evidence of dissolution, maximum widths correspond with vugs that developed along fractures.
- *Openness*: the amount of visible open space in a fracture under the naked eye. We use a Likert-type scale [45] with 5 classes (Table 1) that covers non-uniform ranges in an attempt to account for human bias and the inability to visually quantify the proportion of the fracture that is open. The classes range from 0 (completely filled with cement) to 4 (more than 90% of the fracture is open).
- *Fill type*: describes the different types of cements that can be observed with the assistance of a hand lens. In the case of multiple cement generations, the order in which they are recorded in the spreadsheet represents the relative timing of the cements, from late to early. For example, in box 7 (interval 1915.17–1916.27 m), the numeric codes 1,2 depict two cement generations observed, where the fractures are coated by calcite cement, followed by a lining of bitumen (Figure 2). As this is a general description over a meter-long interval, the fill sequence described here would be the one that is most commonly observed.
- *Distribution*: defines in which third(s) of the core the described features occur. This attribute is an attempt to further refine the vertical distribution of features within a box. For instance, a 1,3 distribution means that the fractures occur in the upper and lower thirds of the interval under consideration; a 1,2,3 distribution implies that fractures occur throughout the entire box.

One advantage of the NMQP approach is that it is highly adaptable. For example, in our experience, we typically have wireline image logs that cover the cored intervals. In such cases, we use the image logs to determine dip and orientation of fractures as a way to optimize our time on the core. Conversely, if image logs do not exist over the cored intervals, then recording orientation and dip information can easily be added to the NMQP workflow; however, time allocation per interval will need to be considered.

2.2.2. Karst Metrics

For this workflow approach, we define karst as either an early epigenic process associated with subaerial exposure and meteoric water or a late hypogenic process during burial that results from acids and fluids decoupled from the overlying surface [46]. Although there is difficultly in differentiating between early meteoric karst features and late burial-related karst features solely from core, there are some key observations that can be made to distinguish the two karst types. For example, meteoric karst features are associated with an exposure horizon in core. Additional lines of evidence for meteoric karst includes the development of touching vugs (i.e., multiple vugs that are connected [42]), the presence of cave deposits, such as speleothems or collapse breccia associated with early fill, and rubble zones associated with karst voids. Evidence of burial karst features can be more challenging to determine in core. Nonetheless, some observations that point to porosity generation during burial include vugs that develop along stylolites or burial fractures, as well as further enlargement of syndepositional fractures and early meteoric karst features.

Because of the time consumption that can happen with detailed differentiation of early and burial karst processes during the NMQP process, we focus efforts on the quantitative geometric description of these features that arise from such processes. Qualitative observations of early versus burial features are recorded as comments. Deciphering of the relative abundance of early versus burial karst comes after the NMQP and requires integration with additional datasets, including a sequence stratigraphic framework, optical petrography, and diagenetic studies [31,37]. The following karst metrics should be collected for each karst type:

- *Count*: number of karst features of a given genetic type that meet the conditions defined by the ground rules. The most common example of karst at the core scale is a combination of isolated dissolution-enhanced voids and touching vugs, reflecting the earliest stages of coastal karst development [47,48], which are often associated with carbonate reservoirs [26–28,37,41,49].
- *Average size*: an estimate of the mean cross-sectional area of the same karst type, which is calculated by multiplying the approximate length of the short and long axes that define each feature.
- *Maximum size*: the maximum measured cross-sectional area of a certain type of karst feature.
- *Openness*: amount of visible open space in a karst features. We use the same Likert-type scale [45] used for fractures.
- *Fill type*: describes the different types of cements that can be observed with the assistance of a hand lens. Rules for fill type reporting and data collection are similar to those described in the case of fractures.
- *Distribution*: similar to the fracture metrics, *distribution* indicates which third(s) of the core contain(s) the features being described.

2.3. Data Processing

The data collection strategy described in the prior section is geared towards this step of the workflow, where information is processed to provide reasonable estimates of non-matrix properties and their vertical variations. The main objective of the data processing step is to deliver a quantitative interpretation of density and porosity associated with the non-matrix pore system. Although there might be a certain degree of uncertainty with respect to the absolute values, this methodology provides early insights on non-matrix variations along the core and in between wells.

Fracture density. The fracture density derived from this workflow yields a P_{21} (as defined by [50]), which is calculated as the summation of all fracture trace lengths (of the same generation) divided by the core surface area:

$$P_{21} = \sum_1^n L / A, \quad (1)$$

where L is fracture trace length, and A is the core surface area.

Fracture porosity. Fracture porosity (P_{22}, [4]) is calculated as the product of the cumulative fracture length multiplied by the characteristic fracture width, minus the amount of pore space occupied by any filling cement:

$$P_{22} = \sum_1^n L \times \alpha \times [1 - f], \quad (2)$$

where L is fracture length, α is characteristic width, and f is the proportion of the fracture filled with cement (defined as the midpoint of the reported interval range). Potential fracture porosity (P_{22pot}) is defined as the porosity that would result from removing all fracture-filling cements (i.e., $f = 0$ in Equation (2)).

Karst porosity. Karst porosity ($\varnothing_k$) is derived from the average vug size multiplied by the number of vugs over a given area:

$$\varnothing_k = \frac{\overline{K_A} \times K_n}{A}(1 - f), \quad (3)$$

where $\overline{K_A}$ is the average vug size, K_n is the total count of vug features, and A is the core surface area. The area should include the slab face area and the area of the core outer surface to account for the vugs in the back of the core. Potential karst porosity ($\varnothing_{kpot}$) is defined as the porosity that would result from removing all filling cements (i.e., f = 0 in Equation (3)). A different approach to estimate karst porosity involves calculating an equivalent radius (based on average vug cross-sectional area) and the volume of the vugs, assuming that they approximate spheres, and therefore taking into account the volume of the core interval. We found that this approach, which is an oversimplification of the vug pore geometry, tends to produce lower porosity numbers than the method in Equation (3). Nonetheless, incorporating both estimations provides a range of karst porosity that can be useful for addressing uncertainty.

3. Results and Discussion

The following section is dedicated to showcasing three examples where NMQP was used to describe core. These cases are not related to each other. They are intended to show how NMQP can be applied in different scenarios. The first case is an example of core from a single well with a variety of non-matrix features that includes both fractures and karst features. The second case is an example of multiple cores wherein epigenic karst is the main diagenetic process, resulting in a high density of vug features with variable vertical distribution. The third case illustrates how to compare NMQP with additional datasets, including borehole acoustic image log and previous fracture interpretation, as well as the beginning of an interval in the well where total losses occurred. We will use these examples as an opportunity to discuss some of the details and direct implications of this methodology for aquifer/reservoir characterization purposes.

3.1. Case 1: Single-Well NMQP

Case 1 represents a detailed example of the NMQP workflow. Figure 4 illustrates the type of dataset that captures the variability expected within carbonate reservoirs. In our experience, carbonate reservoirs can exhibit a range of non-matrix features, whereby some reservoirs are mostly karst-dominated [26], fracture-dominated [51], or a mix of both karst features and fractures [41,52]. This dataset reflects what one can expected to find in core from a carbonate reservoir that has experienced both karst and fracture processes. Figure 4 demonstrates how the NMQP methodology provides a holistic view on the magnitude and distribution of non-matrix features observed in core, which can be compared with numerous datasets, including sedimentary core descriptions, wireline and image logs, and dynamic data, such as production logging tools (PLTs) and well tests. Together, the integration of these datasets provides key insight on the controls driving the total carbonate pore system within a given reservoir [24,26,41]. The following subsections step through the types of observations

and classifications that can be made on the core, as well as what considerations should be made to understand the potential impact of non-matrix features within the reservoir.

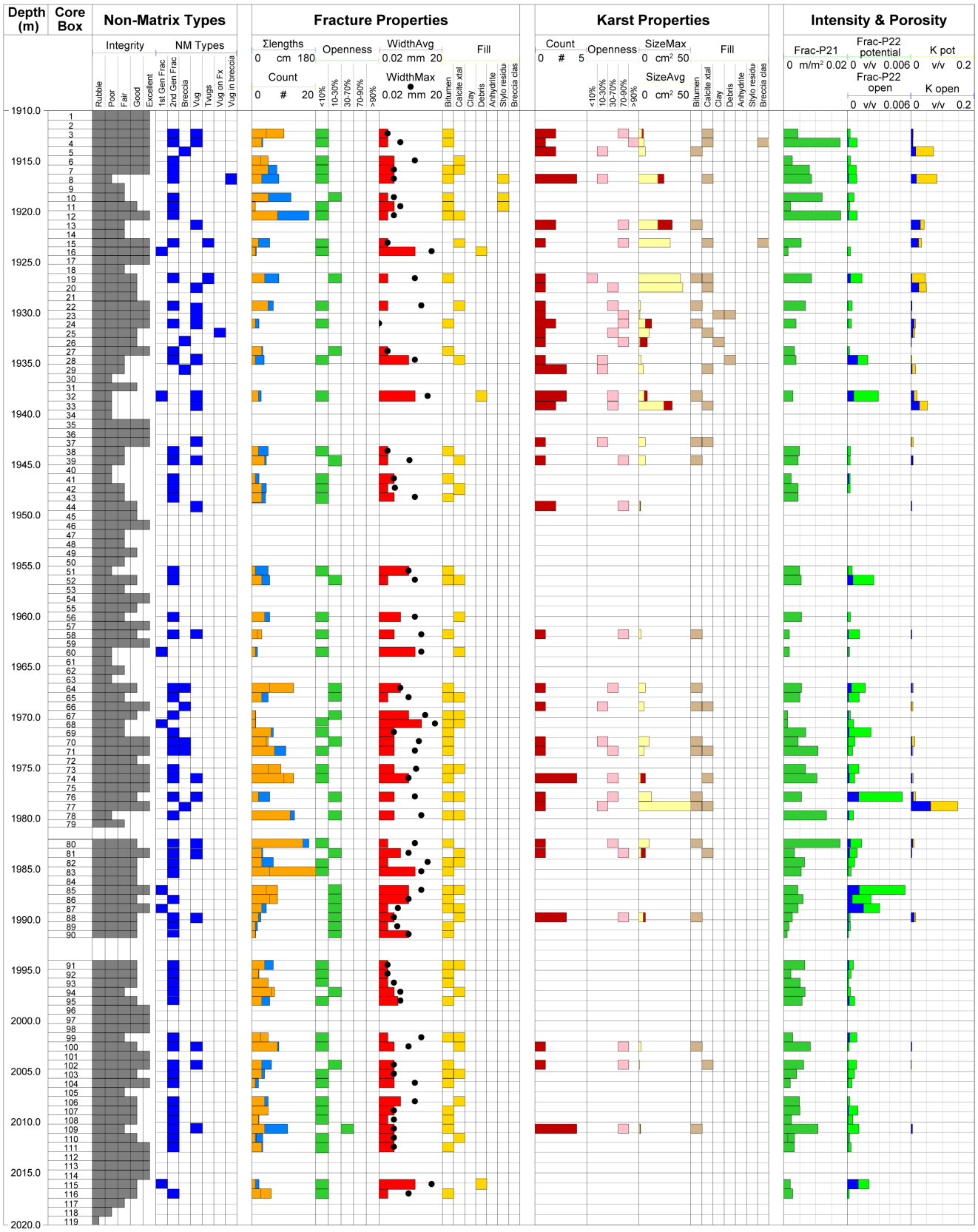

Figure 4. Single well showing the vertical distribution of non-matrix observations obtained with the NMQP methodology.

3.1.1. Core Quality

Results from NMQP show that the overall core quality is good with 88% ranging from fair (22%) to good (31%) to excellent (35%). Only 12% of the core is of poor quality. In reservoirs where non-matrix features are known to exist, missing core and rubble intervals need to be evaluated to determine the cause of little-to-no core recovery. Although drilling operations and wellbore conditions can commonly lead to poor core retrieval, these intervals may reflect non-matrix features, including fracture zones or karst. An evaluation of the core integrity demonstrates 97% core recovery, with two intervals that account for 3.5 m of missing rock from 1981.00 m to 1982.5 m and from 1992.0 m to 1994.0 m. These two missing intervals may indicate non-matrix features, which needs to be corroborated with additional data, such as caliper, image log, or a PLT run showing flow. Our experience has shown that numerous rubble zones and missing intervals are indications of non-matrix features that were previously misinterpreted as the result of coring operations or wellbore integrity (e.g., breakout) during drilling.

3.1.2. Non-Matrix Types

Non-matrix types within this example include a combination of fractures and small-scale dissolution features that can be diagnostic of incipient karst processes. Fractures account for 68% of the observed non-matrix features. We classify fractures based on their relative timing, e.g., syndepositional, early burial, and late burial [34]. Similarly to the proposal of Ibrayev et al. [34], first-generation fractures correspond to fractures that developed contemporaneously with sediment deposition. These fractures often exhibit large apertures ($\geq$1 cm) and are filled with carbonate debris derived from the platform top and early marine calcite cements. Second-generation fractures develop during early burial due to loading and compaction. Such fractures typically have apertures of less than 1 mm and are often associated with stylolites. Late fractures can often be differentiated by cross-cutting relationships with earlier fractures due to continued burial or tectonics.

Breccia accounts for 6% of the observed non-matrix types. Karst-related breccia observed in core typically results from cave collapse or exposure, i.e., epikarst. Dissolved vugs and touching vugs account for 20% and 3% of the observed non-matrix features, respectively. Although such features may not be explicitly defined as karst, e.g., small-scale vugs that have experienced varying degrees of dissolution, their presence provides insight into areas within the reservoir where dissolution may have been favorable for karst development under the right flow conditions. This type of understanding can be extremely useful when predicting where karst processes may impact reservoir properties, such as connected pore volume and high-permeability zones. Consequently, we also flag any vugs that are present within the breccia and along fractures, as such observations may indicate possible flow paths within these features.

3.1.3. Fracture Properties

The fracture properties collected during NMQP include a total count and summation of the total fracture length per box, as well as the degree of open pore volume, average and maximum aperture, and fill material. Per Rule 5, the minimum total sum of fractures > 2 cm in length with apertures $\geq$ 0.05 mm must be at least 10 cm per box.

At 1920 m, core box 12 has eight fractures with a combined total of 160 cm in length (Figure 4). Another core box at 1982 m (core box 80) also has a total fracture length of 160 cm with a fracture count of sixteen. This core box is also next to an interval with no core recovery, whereas there is a box just above the missing core interval at 1979 m with twelve fractures for a total of 120 cm (core box 78). Given the high values of total fracture lengths above and below the missing core interval, additional data should be evaluated to determine whether the interval has any non-matrix features. One straightforward approach would be to examine drilling data to determine whether any losses were recorded during coring at this depth. If so, the volume versus rate (VvR) plot described by Fernández-Ibáñez et al. [52] would be of use, as it utilizes information collected within lost circulation

zones to determine whether the mud losses are due to fractures or karst (see also Case 3 below). If no losses occurred, then an evaluation of image logs would help to determine whether this missing interval is the result of non-matrix features [33].

Second-generation fractures account for 91% of all fractures observed, with 70% of these fractures with an average width in the range of 0.05 to 0.1 mm. The remaining 20% of second -generation fractures have an average width ranging from 0.15 to 0.5 mm. Maximum width is useful to understand the variability of the fracture sets within one box. For example, core box 3 has 40 cm of total fracture length with both an average and maximum width of 0.5 mm. Conversely, core box 32 also has 40 cm of total fracture length, but the average and maximum width are 0.1 mm and 1 cm, respectively, and the number of fractures is less than that observed in core box 3 (Figure 4). Recognizing such variation and distribution of fracture density and width in core can provide insight that can help to address the impact that these features have on variations in non-matrix flow [53].

First-generation fractures account for 9% to the total observed fractures. This type of distribution between first- and second-generation fractures is common in many carbonate reservoirs that we have studied [34]. Although first-generation fractures are often fewer in number compared to second-generation fractures, their commonly wider apertures and vertical extent can have a significant impact on large-scale flow in certain portions of a reservoir [54]. An evaluation of fracture fill material shows that all but one box (core box 109) have less than 30% open pore volume per fracture. Most of the fracture fill is in the form of bitumen and calcite crystals.

3.1.4. Karst Properties

The karst properties collected during NMQP include a count of individual karst features per box, as well as the degree of open pore volume, average and maximum size of each feature, and fill material. According to Rule 5, only vugs that are greater than 1 cm^2 and show evidence of dissolution are recorded, i.e., molds and other isolated pores are excluded. The idea is that vugs that have experienced dissolution are in the earliest stages of karst development. All large karst features, such as caves, start out as small-scale pre-solution openings that include bedding-plane partings, fractures, and/or pores associated with the matrix host rock. Depending on the hydrogeologic conditions under which caves form, the result may be angular or curvilinear conduits, maze-like networks, or meter-scale isolated voids [46]. Although not all vugs that have experienced dissolution are sensu stricto karst, their presence indicates specific locations within the reservoir where karst processes may have occurred beyond what can be explicitly viewed in core. Touching vugs, on the other hand, demonstrate areas where dissolution has progressed enough to generate a well-connected pore system at a local scale, i.e., core.

There are 74 individual karst features observed in the core, with a maximum count of five features in a box. The average and maximum size is about 12 cm^2 and 130 cm^2, respectively. The 130 cm^2 feature is in core box 77 and is a karst breccia that still has an open pore volume estimated at 30%. In core boxes 19 and 20, the observed features are one touching vug and one isolated vug, respectively. Although there is only one feature per box, their proximity and size (about 50 cm^2 each) suggest that sufficient dissolution and fluid flow could have been favorable for karst development within this portion of the reservoir. The degree of open pore volume within the karst features ranges from less than 10% to 90%, with 65% of all features ranging between 25% and 70% open. In our reservoir studies, we have used such observations of open pore volume to guide estimates of field-wide karst porosity [41].

3.1.5. Density and Porosity

Estimates of non-matrix properties and their vertical variations are evaluated through a quantitative interpretation of density and porosity (Equations (1)–(3)). Such values provide an understanding of the potential impact that non-matrix features may have on flow and storativity at the core scale. Fracture density (P_{21}) was calculated using Equation (1).

Fracture density over the entire cored interval has an average of 0.005 fractures/m, with a minimum and maximum density of 0.001 and 0.018 fractures/m, respectively. There are two intervals where density is elevated above the average range: from 1911 m to 1920 m and from 1973 m to 1983 m. Within the interval from 1973 m to 1983 m, the fracture density reaches a maximum above and below a section with missing core (Figure 4), suggesting that the missing section may have resulted from poor core recovery due to the presence of non-matrix features.

Fracture porosity, as estimated here, represents an attempt to capture the range of pore volume associated with fractures as observed in core using Equation (2). The range of pore volume associated with fractures is estimated by observing the amount of open pore volume seen on core (P_{22open}), i.e., accounting for fill within the fractures, and estimating the maximum amount of fracture pore volume, assuming no fill (P_{22pot}). The average values of fracture porosity is a P_{22open} of 0.02% and a P_{22pot} of 0.1%, suggesting that 80% of the fractures are filled mostly with a combination of bitumen and calcite (Figure 4). Maximum values for P_{22open} and P_{22pot} are 0.2% and 0.5%, respectively. Similar to fracture porosity, karst porosity evaluates the range of actual pore volume ($\varnothing_k$) versus maximum possible pore volume ($\varnothing_{kpot}$) associated with karst features in core using Equation (3). The average values for $\varnothing_k$ and $\varnothing_{kpot}$ are 0.9% and 2%, respectively, indicating that only 56% of karst is filled. Maximum values for $\varnothing_k$ and $\varnothing_{kpot}$ are 4% and 15%, respectively. Combined, these average and maximum values of non-matrix porosity provide insight into uncertainty related to pore volume estimates as observed at the core scale.

3.2. Case 2: Using NMQP to Correlate across Wells

NMQP results can also be used to evaluate lateral and vertical trends between wells. In the Case 2 example, NMQP was used to quantify the distribution and porosity associated with the non-matrix features observed in core from a shallow carbonate aquifer. In this case, non-matrix features are in the form of dissolution-enhanced vugs, i.e., karst. Wells in this aquifer are drilled to an average depth of ~25 m, and core is collected in every well with core recovery >95%. Lateral distance between wells ranges from about 0.5 to 1 km.

Figure 5 shows the karst porosity distribution from core collected in seven wells using a common depth scale reference to mean sea level. Vug size and count were used to estimate $\varnothing_k$ and $\varnothing_{kpot}$ for each well. The NMQP results highlight a preferential concentration of vugs around 12 m below mean sea level (m bmsl). There is also an increase in vuggy features below ~20 m bmsl. Whereas the vugs at ~12 m bmsl in most of the cases are open, the features located below ~20 m show a varying degree of openness, which appears to reflect a regional trend. For example, the cluster of wells located in the northern part of the field that run west to east (to the left of Figure 5) show a mostly open, vuggy pore system. Conversely, the cluster of wells in the south part of the field run north to south and shows a vug system that is mostly occluded with cement (Figure 6). We interpret the concentration of vug porosity at two distinct levels as the result of freshwater lens diagenesis. The observations and regional trend derived from NMQP in these wells provide a general framework for describing non-matrix distribution in the aquifer, as well as to impose a decreasing aquifer porosity and permeability trend towards the south.

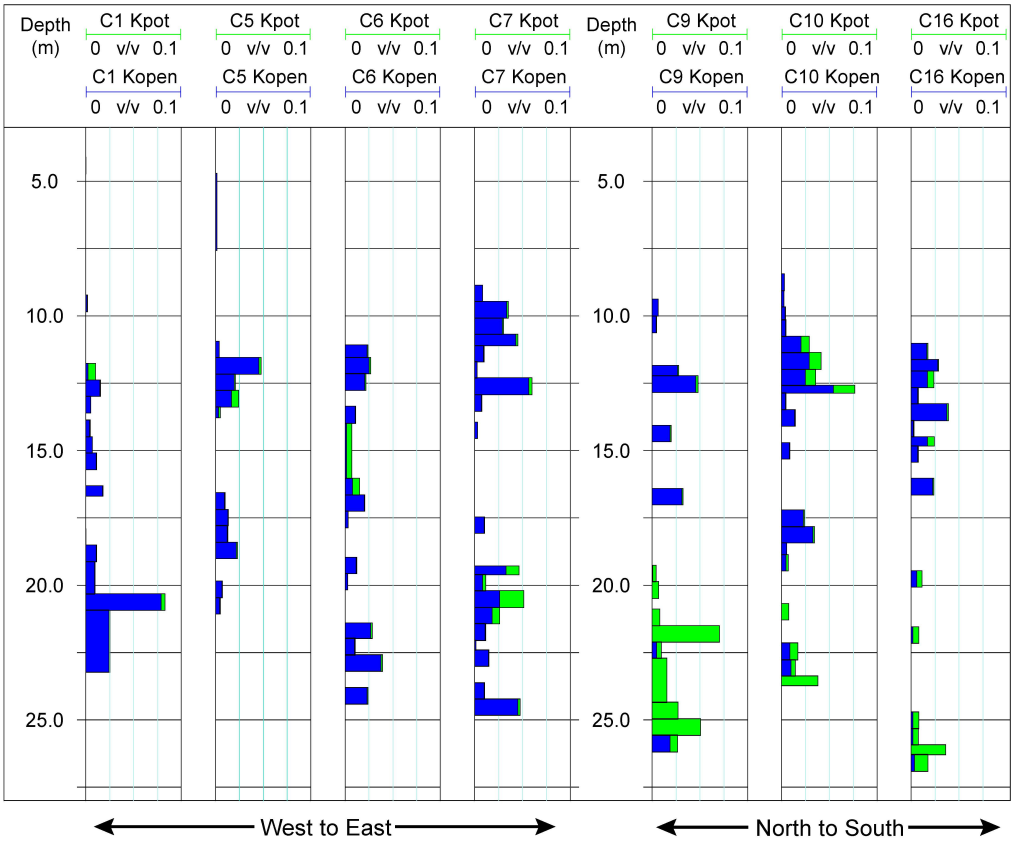

Figure 5. Cross section of multiple wells showing the lateral and vertical distribution of dissolution-enhanced vugs (karst) observed using the NMQP methodology. Attributes displayed correspond to φ22pot and φ22 (Kpot and Kopen, respectively, in log headers), with the well name preceding each of them (e.g., C1 Kpot). The blue fill represents the proportion of vug porosity that is open, and the green fill corresponds to the proportion of vug porosity filled with cements.

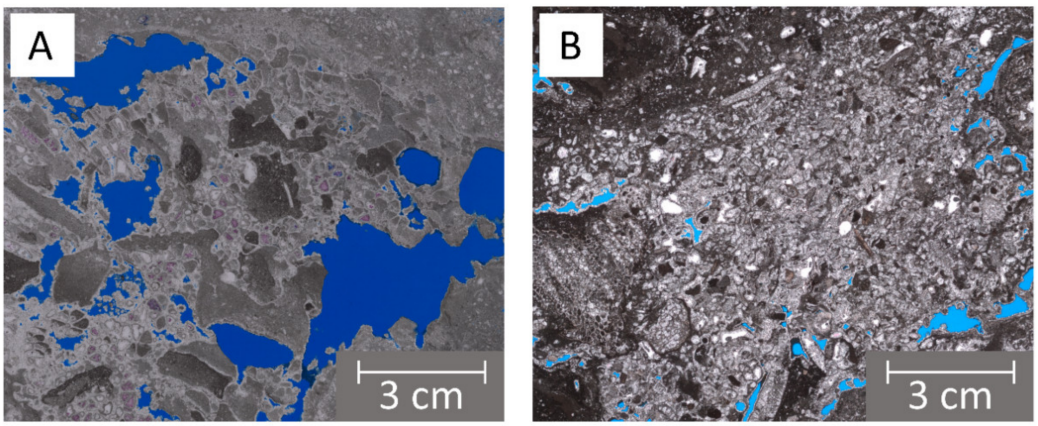

Figure 6. Images showing increase in cementation and decrease in vug size moving from north to south, as shown in Figure 5. Both images are from thin sections collected at 25 m depth from each well. Blue represents porosity. (**A**) Well C9; (**B**) Well C16.

3.3. Case 3: Combining NMQP with Additional Datasets

The integration of NMQP results with additional datasets can provide key insights with respect to how non-matrix features enhance dynamic performance, including mud losses during drilling or flow potential during production. For example, Case 3 shows the results of NMQP over 33 m of core from a carbonate reservoir, which also has a borehole

acoustic image log, associated fracture interpretation from image log, and lost circulation zone (LCZ), where severe losses during drilling started at 5075 m (Figure 7). The fracture interpretation suggests that fractures start where losses initiated, i.e., 5075 m, and continue within the LCZ. Conversely, results from NMQP show the presence of vugs throughout the core, with an increased concentration of vugs starting at 5068 m, where minor losses were recorded, and just above the LCZ, where total losses occurred (Figure 7). Equations (1)–(3) were used to estimate the fracture density and porosity of both fractures and karst. The increase in observed non-matrix features in the core just above and at the start of losses suggests the presence of a well-connected non-matrix pore network that promotes high flow rates. Interpretations using only image logs indicate that fractures alone are the main feature responsible for the losses; however, integration with NMQP clearly demonstrates the occurrence of dissolution-enhanced vugs that also play a role.

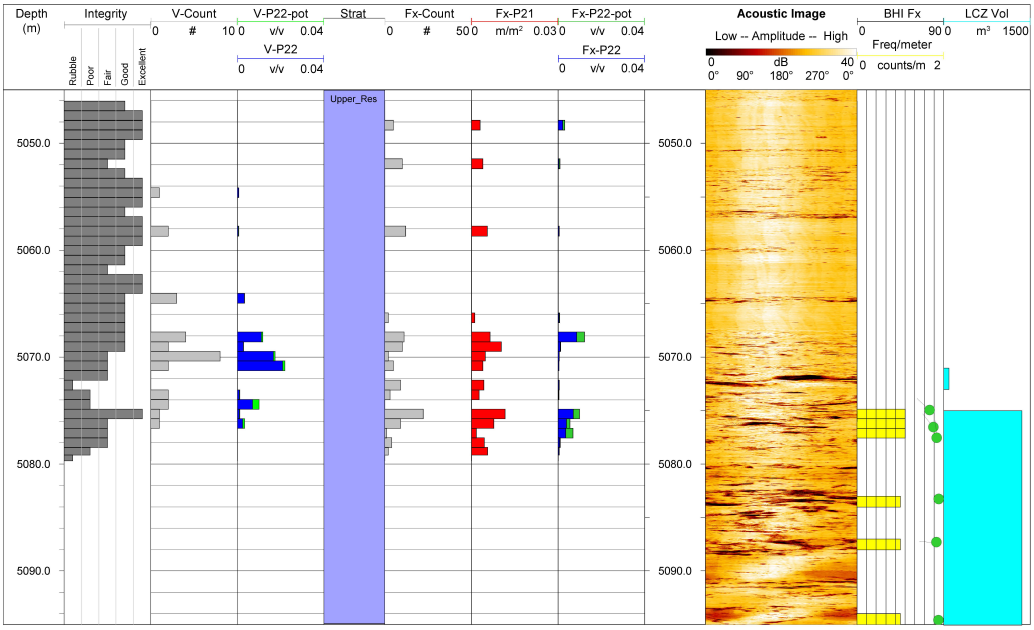

Figure 7. Single well showing the vertical distribution of non-matrix observations using the NMQP methodology compared with additional data, including borehole acoustic image log, fracture interpretation from image, and lost circulation zone (LCZ). From left to right: depth, core integrity, vug count, vug porosity (V-P22) and vug potential porosity (V-P22pot), stratigraphic unit, fracture count (Fx-count), fracture density (Fx-P21), fracture porosity (Fx-P22) and fracture potential porosity (Fx-P22pot), acoustic image log (amplitude), tad poles to image log fracture interpretation and fracture frequency, and top and base of lost circulation zone with volume lost (LCZ). In the vug and fracture potential porosity tracks, the blue fill represents the actual open porosity, and the green represents the proportion of space filled by cements.

Recognizing the difference between fracture and karst development is critical when characterizing reservoirs and developing conceptual models. For example, predicting the magnitude and distribution of fractures away from well control requires an understanding of local and regional paleostress regimes that could be responsible for their development. Conversely, the development of dissolution-enhanced vugs and other karst features require processes including controls on fluid flow and dissolution reactions, which are often tied to exposure horizons and freshwater lens diagenesis. Although karst processes are commonly superimposed on fractures, e.g., dissolution-enhanced fractures, the development of karst pore volume does not require a pre-existing fracture network [47]. Consequently, the integration of multiple datasets, as illustrated in Figure 7, provides insight into the processes responsible for the development of non-matrix features and how to accurately model their presence in the subsurface.

4. Further Applications

The NMQP method provides a fast-pass, semi-quantitative characterization of non-matrix features in core. It requires minimal prior expertise and delivers an integrated approach to extracting basic metrics of both karst features and fractures. NMQP is especially useful in fields with long lengths of core distributed between many wells, as it offers a glance at the types and distribution of non-matrix features. In our experience, this is one of the first tasks to be completed when core is available. The following subsections highlight some benefits and additional applications of the NMQP approach.

4.1. Time Management and Efficiency

Other non-matrix data collection methods, especially those designed for detailed fracture characterization, are typically tedious and time-consuming. Having a NMQP log available first has helped us to target further detailed fracture data collection efforts. Detailed fracture work includes recording properties for individual fractures of all types, lengths, spacing, width, openness, and roughness; as well as exhaustive information on the lithology of the host rock. Although results from such efforts deliver world-class databases used to generate robust statistical inputs to fracture models, the pace at which data is collected is extremely slow, i.e., between 0.5 and 5 m of core described per hour, depending on the complexity of the non-matrix network. When these types of meticulous core descriptions are performed, it is often difficult to decide when a sufficient amount of data has been collected or whether the selected wells are appropriate. Such efforts often result in scope creep and overspending of time and resources.

In our experience, having an available NMQP log provides an opportunity to develop a detailed data collection strategy that allows for targeting of specific intervals in the most representative cored wells. NMQP can help optimize time and resources in situations where business needs typically set a limited time for acquiring core data. For example, consider a case in which we have only one week to characterize 120 m of core. With the standard times per meter reported in Figure 1, one should be able to become familiarized with the main non-matrix core types and complete NMQP within the first few days. This information can then be used then to target detailed data collection in certain intervals of interest (e.g., areas of increased fracture density or areas with a certain type of non-matrix feature). By doing so, we ensure a balanced dataset that contains enough detailed measurements to develop suitable statistical distributions of properties while describing, at a more general level, the non-matrix properties throughout the available core.

4.2. Rapid Data Acquisition and Testing of Concepts

NMQP allows for rapid acquisition of data that can facilitate the testing of concepts in real time, such as by determining whether the presence of increased fracture density represents clusters, corridors, or fault zones. Another example of rapid integration of the NMQP approach is to compare fracture width populations between multiple wells as a proxy for strain. Figure 8 shows an example of how NMQP results can be quickly evaluated to observe differences in fracture widths between wells. In this example not related to any case discussed above, a box plot of fracture widths from four different wells shows that wells B and D have wider fractures, on average, compared to wells A and C (Figure 8). Such differences could be interpreted as variations in the amount of strain experienced by the rocks and thus provide insight into how fracture properties vary spatially within a given reservoir or aquifer.

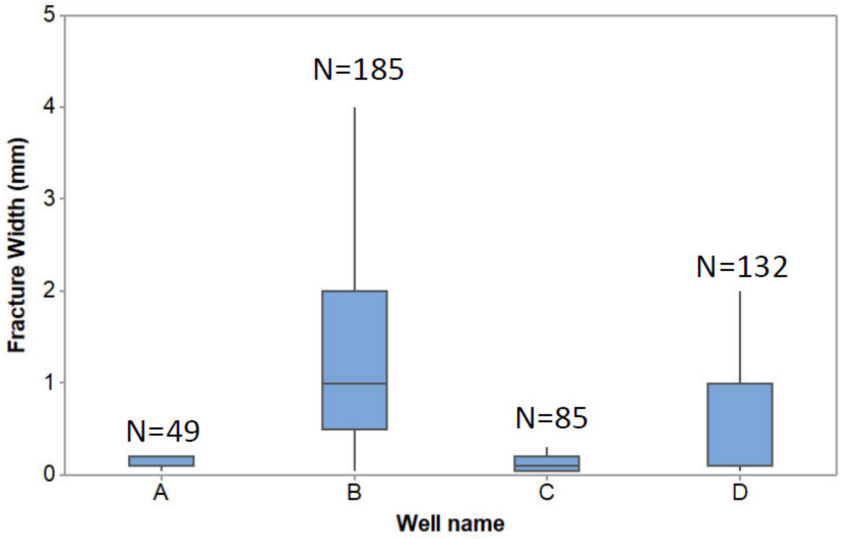

Figure 8. Box plot of fracture widths for four different wells using NMQP data.

NMQP results can also be used test concepts of mechanical stratigraphy. In this situation, the mechanical units can be smaller than the selected interval (core box), in which case the interval could be further subdivided using the *distribution* attribute and compared with sedimentological core descriptions to observe changes in lithology. Additional uses of NMQP results include areal controls on non-matrix density or types, impact of proximity to platform margin, or relations to paleotopography and stratigraphy.

4.3. Input for Numerical Modeling

Data collected with the NMQP approach can also be used to develop early realizations of discrete fracture network (DFN) models, which can later be upgraded with more detailed fracture data collection or calibrated to a well test. Figure 9A shows a cumulative frequency distribution of fracture width constructed using NMQP characteristic width data from 185 core boxes. A similar approach can be employed to model vug distribution (Figure 9B). The collection of width values fits a log-normal distribution (dashed line) that can be use as input for a DFN model (Figure 9).

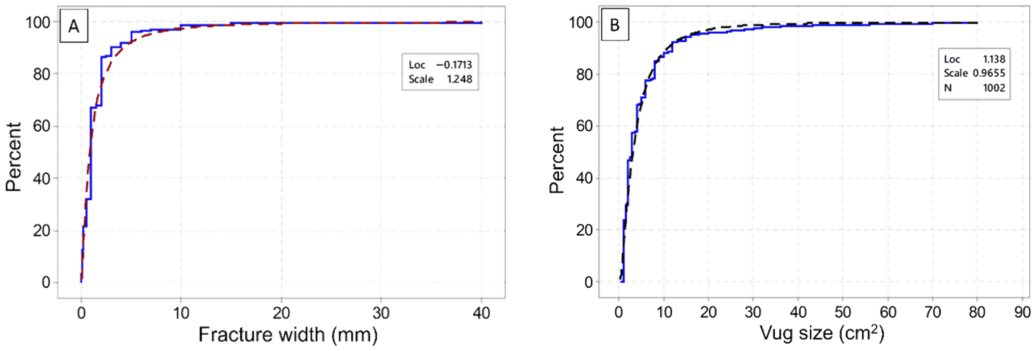

Figure 9. Cumulative frequency distributions of fractures (**A**) and vugs (**B**) based on NMQP of 185 core boxes. Blue lines represent width data collected on core. Dashed lines represent log-normal distributions of widths.

Additionally, carbonate reservoirs with abundant non-matrix features and high-permeability contrast typically require dual-porosity, dual-permeability formulations for more accurate forecast during reservoir simulation and performance prediction. Dual-permeability simulations require a non-matrix porosity input to initialize the models.

NMQP is a reliable source for quantifying non-matrix porosity, not only for the fracture component but for the karst component of the total non-matrix systems.

5. Summary

- NMQP is a comprehensive method for collecting non-matrix (karst and natural fractures) quantitative information in a rapid yet adequate fashion that allows a group of two researchers to describe 12–20 m of core per hour.
- NMQP provides a first-pass approach to understanding non-matrix types and distribution that can be used for reservoir characterization purposes. It also provides useful context for designing and targeting intervals of interest for further detailed data collection.
- NMQP offers enough vertical resolution to define trends and integrate observations with other wellbore data types, such as borehole image logs, losses during drilling, mechanical stratigraphy, or upscaled log properties.
- NMQP-based porosity and density logs provide reasonable values that can be used as input to discrete fracture network models and to initialize dual-porosity, dual-permeability reservoir simulations.

Author Contributions: Initial design and implementation of methodology were jointly performed by P.J.M. and F.F.-I. F.F.-I. developed the data processing step of the methodology. P.J.M. wrote the manuscript with support from F.F.-I. All authors have read and agreed to the published version of the manuscript.

Funding: ExxonMobil Upstream Research Company.

Acknowledgments: The authors thank ExxonMobil Upstream Research Company and ExxonMobil Research, Qatar, for permission to publish this work. We also thank the three anonymous reviewers, who provided constructive feedback, which improved the quality of this manuscript.

Conflicts of Interest: The authors declare that this study received funding from ExxonMobil Upstream Company. The funder was not involved in the study design, collection, analysis, interpretation of data, the writing of this article or the decision to submit it for publication.

References

1. Folk, R.L. *Petrology of Sedimentary Rocks*; Hemphill Publishers: Cedar Hill, TX, USA, 1974; p. 159.
2. Kulander, B.R.; Dean, S.L.; Ward, B.J. *Fractured Core Analysis: Interpretation, Logging, and Use of Natural and Induced Fractures in Core*; American Association of Petroleum Geologists: Tulsa, OK, USA, 1990; Volume 8.
3. Kerans, C.; Tinker, S.W. *Sequence Stratigraphy and Characterization of Carbonate Reservoirs*; SEPM: Broken Arrow, OK, USA, 1997; Volume 40, p. 130.
4. Dershowitz, W.S.; Herda, H.H. Interpretation of Fracture Spacing and Intensity. In Proceedings of the 33rd US Symposium on Rock Mechanics (USRMS), Santa Fe, NM, USA, 3–5 June 1992.
5. Choquette, P.W.; Pray, L.C. Geologic nomenclature and classification of porosity in sedimentary carbonates. *AAPG Bull.* **1970**, *54*, 207–250.
6. Lucia, F.J. Petrophysical parameters estimated from visual descriptions of carbonate rocks: A field classification of carbonate pore space. *J. Pet. Technol.* **1983**, *35*, 629–637. [CrossRef]
7. Lucia, F.J. Rock-fabric/petrophysical classification of carbonate pore space for reservoir characterization. *AAPG Bull.* **1995**, *79*, 1275–1300.
8. Archie, G.E. Classification of carbonate reservoir rocks and petrophysical considerations. *AAPG Bull.* **1952**, *36*, 278–298.
9. Lønøy, A. Making sense of carbonate pore systems. *AAPG Bull.* **2006**, *90*, 1381–1405. [CrossRef]
10. Weger, R.J.; Eberli, G.P.; Baechle, G.T.; Massaferro, J.L.; Sun, Y.F. Quantification of pore structure and its effect on sonic velocity and permeability in carbonates. *AAPG Bull.* **2009**, *93*, 1297–1317. [CrossRef]
11. Skalinski, M.; Kenter, J.A. Carbonate petrophysical rock typing: Integrating geological attributes and petrophysical properties while linking with dynamic behaviour. *Geol. Soc. Lond. Spec. Publ.* **2015**, *406*, 229–259. [CrossRef]
12. Clerke, E.A.; Mueller, H.W., III; Phillips, E.C.; Eyvazzadeh, R.Y.; Jones, D.H.; Ramamoorthy, R.; Srivastava, A. Application of Thomeer Hyperbolas to decode the pore systems, facies and reservoir properties of the Upper Jurassic Arab D Limestone, Ghawar field, Saudi Arabia: A "Rosetta Stone" approach. *GeoArabia* **2008**, *13*, 113–160. [CrossRef]
13. Clerke, E.A. Permeability, relative permeability, microscopic displacement efficiency and pore geometry of M_1 bimodal pore systems in Arab-D limestone. *SPE J.* **2009**, *14*, 524–531. [CrossRef]

14. Anselmetti, F.S.; Luthi, S.; Eberli, G.P. Quantitative characterization of carbonate pore systems by digital image analysis. *AAPG Bull.* **1998**, *82*, 1815–1836.
15. Hollis, C.; Vahrenkamp, V.; Tull, S.; Mookerjee, A.; Taberner, C.; Huang, Y. Pore system characterisation in heterogeneous carbonates: An alternative approach to widely-used rock-typing methodologies. *Mar. Pet. Geol.* **2010**, *27*, 772–793. [CrossRef]
16. Fullmer, S.M.; Guidry, S.A.; Gournay, J.; Bowlin, E.; Ottinger, G.; Al Neyadi, A.M.; Edwards, E. Microporosity: Characterization, distribution, and influence on oil recovery. In Proceedings of the International Petroleum Technology Conference, Doha, Qatar, 19–22 January 2014.
17. Buono, A.; Peterson, K.; Luck, K.; Fullmer, S.; Moore, P.J. Quantitative Digital Petrography: A Novel Approach to Reservoir Characterization. *J. Sediment. Res.* **2019**, *18*, 285–293.
18. Pittman, E.D. Microporosity in carbonate rocks. *AAPG Bull.* **1971**, *55*, 1873–1878.
19. Ahr, W.M. Early diagenetic microporosity in the Cotton Valley Limestone of east Texas. *Sediment. Geol.* **1989**, *63*, 275–292. [CrossRef]
20. Budd, D.A. Micro-rhombic calcite and microporosity in limestones: A geochemical study of the Lower Cretaceous Thamama Group, UAE. *Sediment. Geol.* **1989**, *63*, 293–311. [CrossRef]
21. Loucks, R.G.; Lucia, F.J.; Waite, L.E. Origin and description of the micropore network within the lower Cretaceous Stuart City Trend tight-gas limestone reservoir in Pawnee Field in South Texas. *Gulf Coast Assoc. Geol. Soc.* **2013**, *2*, 29–41.
22. Lucia, F.J.; Loucks, R.G. Micropores in carbonate mud: Early development and petrophysics. *Gulf Coast Assoc. Geol. Soc.* **2013**, *2*, 1–10.
23. Kaczmarek, S.E.; Fullmer, S.M.; Hasiuk, F.J. A universal classification scheme for the microcrystals that host limestone microporosity. *J. Sediment. Res.* **2015**, *85*, 1197–1212. [CrossRef]
24. Fullmer, S.; Al Qassab, H.; Buono, A.; Gao, B.; Kelley, B.; Moore, P.J. Carbonate pore-system influence on hydrocarbon displacement and potential recovery. *J. Sediment. Res.* **2019**, *18*, 268–284.
25. Tinker, S.W.; Ehrets, J.R.; Brondos, M.D. Multiple karst events related to stratigraphic cyclicity: San Andres Formation, Yates field, west Texas. In *Unconformities and Porosity in Carbonate Strata*; Budd, D.A., Saller, A.H., Harris, P.M., Eds.; AAPG Memoir: Tulsa, OK, USA, 1995; Volume 63, pp. 213–238.
26. Ahdyar, L.O.; Sekti, R.P.; Mohammad, S.R.; Fernandez-Ibanez, F.; Moore, P.J. *Integrated Carbonate Non-Matrix Characterization in Banyu Urip Field*; Indonesian Petroleum Association: South Jakarta, Indonesia, 2019.
27. Craig, D.H. Caves and other features of Permian karst in San Andres dolomite, Yates field reservoir, west Texas. In *Paleokarst*; James, N.P., Choquette, P.W., Eds.; Springer: Berlin/Heidelberg, Germany, 1988; pp. 342–363.
28. Kerans, C. Karst-controlled reservoir heterogeneity in Ellenburger Group carbonates of west Texas. *AAPG Bull.* **1988**, *72*, 1160–1183.
29. Lorenz, J.; Hill, R. Measurement and analysis of fractures in core. In *Geological Studies Relevant to Horizontal Drilling: Examples from Western North America*; Schmoker, J.W., Coalson, E.B., Brown, C.A., Eds.; Association of Geologists: Denver, CO, USA, 1992; pp. 47–57.
30. Loucks, R.G. Paleocave carbonate reservoirs: Origins, burial-depth modifications, spatial complexity, and reservoir implications. *AAPG Bull.* **1999**, *83*, 1795–1834.
31. Heward, A.P.; Chuenbunchom, S.; Mäkel, G.; Marsland, D.; Spring, L. Nang Nuan oil field, B6/27, Gulf of Thailand: Karst reservoirs of meteoric or deep-burial origin? *Pet. Geosci.* **2000**, *6*, 15–27. [CrossRef]
32. Lorenz, J.C.; Cooper, S.P. *Atlas of Natural Fractures and Coring-Induced Structures in Core*; John Wiley & Sons: Hoboken, NJ, USA, 2017; p. 320.
33. Fernández-Ibáñez, F.; DeGraff, J.M.; Ibrayev, F. Integrating borehole image logs with core: A method to enhance subsurface fracture characterization. *AAPG Bull.* **2008**, *102*, 1067–1090. [CrossRef]
34. Ibrayev, F.; Fernandez-Ibanez, F.; DeGraff, J.M. Using a genetic-based approach to enhance natural fracture characterization in a giant carbonate field. In Proceedings of the SPE Annual Caspian Technical Conference & Exhibition, Astana, Kazakhstan, 1–3 November 2016.
35. Tonkins, M.C.; Coggan, J.S. Characterization of Rock Fracturing for Vertical Boreability. *Procedia Eng.* **2017**, *191*, 112–118. [CrossRef]
36. Kerans, C.; Donaldson, J.A. Proterozoic paleokarst profile, Dismal Lakes Group, NWT, Canada. In *Paleokarst*; Springer: Berlin/Heidelberg, Germany, 1988; pp. 167–182.
37. Ronchi, P.; Ortenzi, A.; Borromeo, O.; Claps, M.; Zempolich, W.G. Depositional setting and diagenetic processes and their impact on the reservoir quality in the late Visean–Bashkirian Kashagan carbonate platform (Pre-Caspian Basin, Kazakhstan). *AAPG Bull.* **2010**, *94*, 1313–1348. [CrossRef]
38. Lockman, D.F.; George, R.P.; Hayes, M.J. *A Systematic Technique for Describing and Quantifying Fractures in Cores. MP-44*; The Pacific Section American Association of Petroleum Geologists: Bakersfield, CA, USA, 1997; pp. 1–33.
39. DeGraff, J.M.; (ExxonMobil (retired), Spring, TX, USA). Personal communication, 2018.
40. Watkins, H.; Bond, C.E.; Healy, D.; Butler, R.W. Appraisal of fracture sampling methods and a new workflow to characterise heterogeneous fracture networks at outcrop. *J. Struct. Geol.* **2015**, *72*, 67–82. [CrossRef]
41. Fernández-Ibáñez, F.; Moore, P.J.; Jones, G.D. Quantitative assessment of karst pore volume in carbonate reservoirs. *AAPG Bull.* **2019**, *103*, 1111–1131. [CrossRef]

42. Lucia, F.J. Touching Vug Reservoirs. In *Carbonate Reservoir Characterization, An Integrated Approach*; Lucia, F.J., Ed.; Springer: Berlin/Heidelberg, Germany, 2007; pp. 301–331.
43. Fernández-Ibáñez, F.; Jones, G.D.; Mimoun, J.G.; Bowen, M.G.; Simo, J.A.; Marcon, V.; Esch, W.L. Excess permeability in the Brazil pre-Salt: Nonmatrix types, concepts, diagnostic indicators, and reservoir implications. *AAPG Bull.* **2022**, *106*, 701–738. [CrossRef]
44. Ortega, O.J.; Marrett, R.A.; Laubach, S.E. A scale-independent approach to fracture intensity and average spacing measurement. *AAPG Bull.* **2006**, *90*, 193–208. [CrossRef]
45. Likert, R. A technique for the measurement of attitudes. *Arch. Psychol.* **1932**, *22*, 1–55.
46. Palmer, A.N. Origin and morphology of limestone caves. *Geol. Soc. Am. Bull.* **1991**, *103*, 1–21. [CrossRef]
47. Vacher, H.L.; Mylroie, J.E. Eogenetic karst from the perspective of an equivalent porous medium. *Carbonates Evaporites* **2002**, *17*, 182–196. [CrossRef]
48. Breithaupt, C.I.; Gulley, J.D.; Moore, P.J.; Fullmer, S.M.; Kerans, C.; Mejia, J.Z. Flank margin caves can connect to regionally extensive touching vug networks before burial: Implications for cave formation and fluid flow. *Earth Surf. Processes Landf.* **2021**, *46*, 1458–1481. [CrossRef]
49. Kosters, M.; Hague, P.F.; Hofmann, R.A.; Hughes, B.L. Integrated modeling of karstification of a central Luconia Field, Sarawak. In *IPTC 2008: International Petroleum Technology Conference 2008*; European Association of Geoscientists & Engineers: Houten, The Netherlands, 2008; p. cp-148.
50. Van Dijk, J. Analysis and Modeling of Fractured Reservoirs. In Proceedings of the European Petroleum Conference, SPE-50570-MS, The Hague, The Netherlands, 20–22 October 1998. [CrossRef]
51. Belfield, W.C. Characterization of a Naturally Fractured Carbonate Reservoir: Lisburne Field, Prudhoe Bay, Alaska. In Proceedings of the SPE Annual Technical Conference and Exhibition, Houston, TX, USA, 2–5 October 1988. [CrossRef]
52. Fernandez-Ibanez, F.; DeGraff, J.M.; Moore, P.J.; Ahdyar, L.; Nolting, A. Characterization of non-matrix type and flow potential using lost circulation information. *J. Pet. Sci. Eng.* **2019**, *180*, 89–95. [CrossRef]
53. Bisdom, K.; Bertotti, G.; Nick, H.M. The impact of different aperture distribution models and critical stress criteria on equivalent permeability in fractured rocks. *J. Geophys. Res. Solid Earth* **2016**, *121*, 4045–4063. [CrossRef]
54. Odling, N.E.; Gillespie, P.; Bourgine, B.; Castaing, C.; Chiles, J.P.; Christensen, N.P.; Watterson, J. Variations in fracture system geometry and their implications for fluid flow in fractures hydrocarbon reservoirs. *Pet. Geosci.* **1999**, *5*, 373–384. [CrossRef]